PCCP

Carotenoids Promote Lateral Packing and Condensation of Lipid Membranes

Journal:	*Physical Chemistry Chemical Physics*
Manuscript ID	CP-ART-02-2020-001031.R1
Article Type:	Paper
Date Submitted by the Author:	02-May-2020
Complete List of Authors:	Mostofian, Barmak; Oregon Health & Science University, Johnson, Quentin; Berry College Smith, Jeremy; Oak Ridge National Laboratory, UT/ORNL Center for Molecular Biophysics Cheng, Xiaolin; Ohio State University

Carotenoids Promote Lateral Packing and Condensation of Lipid Membranes

Barmak Mostofian[1,*], Quentin R. Johnson[1,2], Jeremy C. Smith[1,3], and Xiaolin Cheng[1,**,***]

(1) Center for Molecular Biophysics, Oak Ridge National Lab, Oak Ridge, TN 37830, USA

(2) Berry College, 2277 Martha Berry Hwy NW, Mt Berry, GA, 30149 USA

(3) Department of Biochemistry and Cellular & Molecular Biology, University of Tennessee, Knoxville, TN 37996, USA

*Current affiliation: Department of Biomedical Engineering, School of Medicine, Oregon Health and Science University, Portland, OR 97239, USA

**Current affiliation: College of Pharmacy, Biophysics Graduate Program, Translational Data Analytics Institute, The Ohio State University, Columbus, OH 43210, USA

***E-mail: cheng.1302@osu.edu

Abstract

Carotenoids are pigment molecules that protect biomembranes against degradation and may be involved in the formation of functional bacterial membrane microdomains. Little is known on whether different types of carotenoids have different effects on the membrane or if there is any concentration dependence of these effects. In this work, we present results from molecular dynamics simulations of phospholipid bilayers containing different amounts of either β-carotene or zeaxanthin. Both β-carotene and zeaxanthin show the ability to laterally condense the membrane lipids and reduce their inter-leaflet interactions. With increasing concentrations, both carotenoids increase the bilayer thickness and rigidity. The results reveal that carotenoids have similar effects as cholesterol on regulating the behavior of fluid-phase membranes, suggesting that they could function as sterol substitutes and confirming their potential role in the formation of functional membrane domains.

Introduction

Biological membranes form the interfaces between the interiors of cells and their outside environments and thus play a key role in intercellular communication and molecular transport.[1] They provide an ideal multicomponent environment harboring a variety of lipids, proteins, and other additives,[2-5] that can laterally segregate and lead to the coexistence of immiscible liquid phases.[6-8] The separation of lipids into liquid ordered (Lo) and liquid disordered (Ld) phases is hypothesized to be responsible for the formation of functional domains, or "lipid rafts", in eukaryotic cell membranes.[9]

Additives can have a strong effect on a membrane's properties. For instance, sterols, which occur in vertebrate, plant, and fungal membranes, provide firmness and integrity to the membrane while keeping it fluid.[10-14] Cholesterol, the major component of mammalian cell membranes, is essential for membrane fusion,[15] signal transduction, and membrane protein function.[16-17] Importantly, sterols preferably pack themselves with specific types of lipids, such as fully-saturated acyl chains or sphingolipids, thus facilitating the formation of Lo states that have distinct physical properties from the surrounding membrane region.[18-19]

Carotenoids are another type of additive vital for membrane function.[20-21] Carotenoids are organic pigments with an innate light-harvesting ability. They serve as antenna molecules expanding the spectrum of light accessible to chlorophylls in photosynthesis[22-25] and as bioprotective molecules against excessive light and oxidative damage.[26-27] Most naturally occurring carotenoids are polyisoprenoids with a conjugated chain of double bonds biosynthesized by plants or micro-organisms.[28] Once ingested by animals, carotenoids can photoprotect the retinas of their eyes or neutralize reactive oxygen

species (ROS), such as free radicals, which cause damage to the cell.[29-31] Their antioxidant properties are reported to have several clinical benefits to humans.[32-37] Notably, the incorporation of carotenoids into cell membranes helps protect the membrane lipids, of which polyunsaturated fatty acid chains are particularly vulnerable to ROS attack.[38-39]

Recently, the presence of carotenoids in prokaryotic membranes has also been associated with the formation of functional microdomains in bacteria. Lopez et al. have shown that bacterial membranes may contain regions that, similar to rafts in eukaryotic cells, resist detergent solubilization, contain raft-associated recruiting proteins as well as other proteins essential for membrane trafficking, and are enriched in polyisoprenoids, such as squalene or carotenoids.[40-43] These noncyclic terpenoids can confer rigidity to the membrane regions they reside in and may thus have a similar packing effect on lipid membranes as their cyclic counterpart, cholesterol, in animal cell membranes.

The effect of carotenoids on membrane properties has been studied by a variety of biophysical techniques. Diffraction measurements have shown that carotenoids tend to adopt an extended conformation in a lipid bilayer[44-45] and that oxygen-containing carotenoids, or xanthophylls, have a greater disturbing effect on the polar region of phospholipids than do their counterparts, carotenes, which lack oxygen.[46] Moreover, NMR, EPR and permeability experiments revealed that the presence of membrane-spanning carotenoids increases the rigidity and stability of membranes and reduces their permeability to ions and molecular oxygen.[47-50] In light of these findings, it is desirable to know how carotenoid molecules interact with membrane lipids to induce the above-mentioned effects and whether their manifestation depends on the amount of carotenoids present.

Molecular dynamics (MD) simulation is an excellent tool to investigate the molecular interactions between the different components in a lipid membrane and to assess their overall effect on the membrane. For example, previous MD studies have shed light on how membrane lipids can cluster or form domains[51-53] and how curvature and leaflet asymmetry influence their organization.[5, 54-58] In particular, the condensation effect of cholesterol on biomembranes has been investigated extensively.[59-63]

In contrast, far fewer simulations of carotenoids in membranes have been reported.[64-67] In one such study, Cerezo et al. analyzed the conformations of different carotenoids and concluded that the presence of hydroxyl groups in zeaxanthin "anchors" the carotenoid to the bilayer polar head groups, whereas β-carotene, that lacks a hydroxyl group, can rotate more freely within the bilayer.[65] Grudzinski et al. combined MD simulations with imaging experiments to show that xanthophylls are preferably tilted with respect to the bilayer normal and that this slightly tilted orientation is stabilized by hydrogen bonds.[66] More recently, we have shown how relatively high concentrations of carotenoids can promote the vertical compression of membranes by two different mechanisms: in the Lo phase, lipid tails bend and compress in both bilayer leaflets, whereas, in the Ld phase, the lipid tails from opposing leaflets interdigitate.[67] However, details on how the structural and mechanical properties of the membrane are altered with increasing carotenoid concentrations remain unknown.

In the current study, we examine the effects of β-carotene and zeaxanthin (Figure 1) on biomembranes by analyzing MD simulations of the two carotenoids at different concentrations in a bilayer of 1-palmitoyl-2-oleoyl-sn-glycero-3-phosphocholine (POPC). Although the pure POPC membrane composition is more simplistic than that of multi-

component cell membranes, this single-lipid membrane model is often used when the effect of extrinsic molecules or materials on a bilayer is analyzed.[68-70] The present results reveal that carotenoids have a condensation effect on the membrane structure. Both β-carotene and zeaxanthin increase the lateral packing of lipids, thus making the membrane thicker and stiffer. At high concentrations, this effect is more pronounced in the presence of β-carotene than zeaxanthin as the latter can form simultaneous hydrogen bonds with the lipid molecules in opposing leaflets, thus holding them together. At low concentrations, on the other hand, β-carotene can flip around the membrane midplane and cause localized distortions in lipid tail conformation, leading to a less rigid membrane structure. The results highlight how the bilayer-spanning carotenoids can mimic the effects of sterols on membrane structure, thus functioning as a "surrogate" for cholesterol and possibly facilitating the formation of functional membrane domains.

Methods

System setup and simulation

All-atom MD simulations were performed on planar bilayer membrane models of POPC that contain different concentrations of either β-carotene or zeaxanthin. The membrane models consist of 200 POPC molecules per leaflet and 4, 10, 20, or 40 membrane-spanning carotenoid molecules, which correspond to molar carotenoid concentrations of 1%, 2.5%, 5% and 10%, respectively. The 10% molar concentration corresponds to the maximum solubility reported for zeaxanthin.[71]

All bilayer models were assembled with the PACKMOL software package,[72] first preparing a small bilayer with 10 POPC lipids in each leaflet before inserting 0, 1, or 2 membrane-spanning carotenoids into it. These small bilayer patches formed the building blocks of the actual simulation starting systems, and they were translated 5 times along the x-axis and 4 times along the y-axis and combined to yield a system with 200 POPC lipids per leaflet and 4, 10, 20, or 40 membrane-spanning carotenoid molecules (see Figure S1). During the equilibration simulations (>100 ns), the initially relatively inhomogeneous membrane structure relaxes in the x-y plane and along the z-axis independently, with lipids from opposite leaflets interdigitating, and lipids and carotenoids mixing with each other.

In order to assess the effect of carotenoids on membranes, a pure POPC bilayer of the same size was simulated with no carotenoids added. An ether lipid (di-palmitoyl-phosphatidylcholine) bilayer of the same size with 10 mol% zeaxanthin was also simulated to analyze roles of carbonyl oxygens at the bilayer interface in phospholipid–zeaxanthin interactions. The bilayers were solvated with TIP3P[73] water molecules, resulting in a total of ~55,000 atoms in each system.

The CHARMM36 lipid force field[74-75] was used along with carotenoid parameters previously determined by Cerezo et al.[65] and recently derived parameters for the ether lipid simulations.[76] For each system, atomic coordinates were first minimized using the conjugate gradient algorithm for 2000 steps, followed by simulations in the constant particle number, pressure, and temperature (NPT) ensemble with a semi-isotropic pressure coupling that allows the z-axis to expand and contract independently from the x-y plane.[77] The systems were first heated to 300 K within 5 ns using a 1 fs time step and applying dihedral restraints to the carotenoids to ensure a planar starting structure of the conjugated

double bond chains. This was followed by 500 ns of simulations without restraints using a 2 fs time step. The first 100 ns were used as equilibration and the remaining 400 ns were used for analysis. Although properties such as lipid demixing and phase separation of biomembranes take place on a ms time scale,[7] this study mainly focuses on local interactions between carotenoids and phospholipids, which are known to occur on the order of 100s of ns.[65]

Langevin dynamics[78] were used to control the temperature at 300 K with a damping coefficient of 2/ps. This stochastic thermostat allows to maintain the system's temperature by adding friction and random force terms to the equations of motion, thus reducing any artifacts that may arise from some commonly-used weak-coupling thermostats. We used the Langevin piston method[79] to keep the pressure at 1 atm. Van der Waals (vdW) interactions were truncated via a force-based switching function with a switching distance of 8 Å and a cutoff distance of 12 Å. Short-range Coulomb interactions were cut off at 12 Å, long-range electrostatic interactions were calculated using the Particle-Mesh Ewald summation[80-81]. Bonds to hydrogen atoms were constrained using the SHAKE algorithm.[82] The simulation parameters are summarized in the SI. All simulations were performed using NAMD 2.9[83] on the supercomputing resources of the National Energy Research Scientific Center (NERSC) and the Oak Ridge Leadership Computing Facility (OLCF).

Simulation analysis

The bilayer thickness, D_B, was derived as the distance between the average z-coordinates of the choline's nitrogen and three methyl carbons from one bilayer leaflet to the other. The area per lipid, ApL, is the average x-y plane area of the bilayer divided by the number

of POPC molecules per leaflet plus the number of carotenoids present. The carbon tetrahedral order parameter of lipids, S_{CH}, is defined as

$$S_{CH} = \frac{\langle 3\cos^2\alpha - 1 \rangle}{2} \quad (1)$$

where α is the angle between the acyl chain C-H bond and the bilayer normal[84] and the angular bracket indicates the ensemble average for a specific C-H bond. Individual lipid tilts were measured as the angle, δ, between a lipid's head-to-tail vector and the bilayer normal of the leaflet containing the lipid under consideration. The lipid head-to-tail vector connects the center position of the head group's phosphate and glyceride C2 atom with the center position of the three terminal carbon atoms on the POPC acyl chains. Similarly, for each carotenoid molecule the rotation angle, Θ, was derived between the bilayer normal and the line connecting the centers of mass of the carbon atoms at both halves of the conjugated chain, as was done in previous studies.[65-66]

The membrane bending modulus, k_m, was estimated from the contributions of the individual lipid pairs to bilayer deformation, derived from their tilt and splay angles as previously described.[85] The splay angle of a lipid, γ, is the angle its head-to-tail vector forms with the head-to-tail vector of a surrounding lipid within 10 Å. For small splay angles ($\gamma < 20°$) of individual lipids with tilt angles $\delta < 10°$, the two-molecule potential of mean force (PMF) for splay is given by $PMF(\gamma) = -k_B T ln[P(\gamma)/\sin(\gamma)]$, where P(γ) is the probability distribution density of γ. With the splay deformation energy being $\sim\frac{1}{2}\chi_{ij}\gamma^2$ at small splay angles, we obtained the splay modulus χ_{ij} from the slope by fitting $PMF(\gamma)$ vs. γ^2. The bending modulus was then derived as

$$\frac{1}{k_m} = \frac{1}{N}\sum_{i,j}\frac{n_{ij}}{\chi_{ij}} \quad (2)$$

where n_{ij} is the number of (i,j) pairs and $N = \sum_{i,j} n_{ij}$ is the total number of possible lipid pairs.

In-plane mean-square displacements (MSDs) were calculated for all lipids as $\langle r(t)^2 \rangle = \langle (r(t_0 + t) - r(t_0))^2 \rangle$, where $r(t)$ are the x- and y-coordinates of the head group phosphorous atoms after a time interval t and the angular brackets indicate time and ensemble averages. The MSDs were evaluated at every recorded time step, i.e., Δt_0 = 4 ps, and up to a maximum time interval of t = 100 ns. For each system, the anomalous diffusion coefficient (D_α) and the anomalous diffusion exponent (α, with $0 < \alpha < 1$) were obtained for 10 ns $\leq t \leq$ 50 ns from two-parameter nonlinear fits to the MSD with $\langle r(t)^2 \rangle = 4D_\alpha t^\alpha$, as described elsewhere.[86-87]

Average values were calculated over four blocks of 100 ns of simulation time, with the exception of the MSDs, which, in order to provide good statistics at long time intervals, were calculated over 400 ns of simulation time for each lipid and average values were obtained over four blocks of 100 individual lipids. Error bars are the 95% credibility region derived from a 1000-fold Bayesian bootstrap resampling procedure.[88] All analysis was performed with the VMD software.[89]

Results and Discussion

Carotenoids condense the lipid bilayer

One of the key structural properties of biomembranes is its thickness, which can be easily obtained from simulations and compared to results from scattering experiments.[90] Figure 2A shows how the bilayer thickness (D_B) increases with increasing carotenoid concentrations. In the presence of β-carotene, in particular, the thickness changes from 41.7 +/- 0.04 Å in the pure POPC membrane to 43.4 +/- 0.11 Å at 10 mol%. This increase may seem small, but, as the non-overlapping error bars of bilayer thickness at the higher carotenoid concentrations indicate, the calculation is precise and the trend toward a thicker membrane at greater carotenoid concentrations is statistically significant. D_B for the pure POPC model is in reasonable agreement with values derived from simultaneous X-ray and neutron scattering data (D_B = 39.9 Å +/- 0.8 Å).[91] The continuous thickening of POPC membranes with carotenoid concentration is an interesting result because it shows how the lipid membrane's thickness can be fine-tuned by adding a certain amount of carotenoids.

The pure POPC bilayer has an average surface area per lipid (ApL = 65.5 +/- 0.05 $Å^2$), in good agreement with the corresponding experimental value (ApL = 64.2 +/- 1.3 $Å^2$).[91] The ApL is a membrane property that normally displays an opposite trend to the thickness: thus, as expected, the presence of carotenoids leads to a reduction of the ApL, and more so for β-carotene than for zeaxanthin (Figure 2B). The increase in D_B and decrease of ApL suggest that the carotenoids exhibit a condensation effect on the lipid membrane akin to that of sterols. In fact, the values of D_B and ApL at a carotenoid concentration of 10 mol% agree favorably with those from previously reported POPC-membrane experiments and simulations with the same concentration of cholesterol (D_B = 42-44 Å and ApL = 58-60 $Å^2$).[92-94]

Changes in bilayer thickness can originate from different types of interactions between the two membrane leaflets, with significant implications for the function of a membrane as shown in numerous previous studies on inter-leaflet coupling and (anti-)registration.[56, 95-97] Essentially, the carotenoids couple the two leaflets by virtue of spanning them and the interdigitation of the opposing acyl chains is a measure of the degree of inter-leaflet interaction. This interdigitation can be quantified by the overlap of the localization probability densities of opposing chains. Such density profiles along the bilayer normal (z-)axis are shown in Figures 3B and C for different functional groups of the POPC lipids and β-carotene at 10 mol% (see colored groups in Figure 3A). The degree of interdigitation, i.e., the overlapping integral of the opposing acyl chain density functions, $P_{overlap}$, is highlighted in Figure 3C. The decrease of this overlap with increasing carotenoid concentration (Figure 2C) means that the carotenoids, and in particular β-carotene, reduce the interdigitation of the two membrane leaflets, which is consistent with the overall increase in membrane thickness.

The acyl chain order parameter is a property that is also related to the bilayer thickness and area per lipid[98-100], reflecting the dynamics and the packing of lipids.[101] Figure 4 shows the carbon tetrahedral order parameter, S_{CH}, for individual carbon atoms of both POPC acyl chains as a function of β-carotene concentration (the zeaxanthin simulations resulted in similar profiles; data not shown). The distinct shapes of these two profiles are characteristic of the POPC lipid with one double bond in the *sn*-2 chain.[84] The magnitude of S_{CH} slightly increases with the carotenoid concentration (Figure 2D) in accord with the increase in membrane thickness, since more ordered lipids can pack more tightly and lead to thicker membranes.

The ability to change the overall thickness, the inter-leaflet interactions, or the lateral packing is a feature of elastic lipid membranes.[102-104] The rigidity of lipid bilayers, i.e., their resistance against curvature formation, depends on the packing of the individual lipid components. Thus, the local curvature of a membrane is intimately connected to the tilt and splay of individual lipids.[105-106] Figure 5A shows the distribution of POPC tilt angles, δ, with respect to the corresponding leaflet normal. The number of lipids with δ >20° decreases exponentially in all systems suggesting that the lipids are fairly immobile. Despite the average tilt angle being relatively small in the membrane (δ = ~20°), localized large tilting of lipids with respect to neighboring lipids, referred to as the splay angle, can still occur, which gives rise to small membrane undulations. The distribution of splay angles describes local membrane rigidities and can be used to derive an average bending modulus, k_m, according to equation (2). The membrane becomes more rigid with a growing concentration of carotenoids as depicted in Figure 5B, indicating that the packing of carotenoids around lipid molecules influences the tilt and splay angles of lipids. The more rigid membranes are also manifested by an increase in thickness and a decrease in surface area per lipid as well as increased lipid order,[107] illustrating the connection between the lateral condensation and the rigidity of a membrane. Interestingly, the values found here for the membrane bending modulus at 10 mol% (k_m = ~9.5 k_BT) are somewhat smaller than with the same amount of cholesterol in POPC bilayers (k_m = ~20 k_BT), as determined by neutron spin echo and dynamic light scattering and from MD simulations[106, 108-109], suggesting that the polyene chain structure in carotenoids is more flexible and thus weaker in impairing membrane elasticity than the four-fused-ring moiety in cholesterol.

To analyze the effects of carotenoids on the lipid dynamics, we evaluated their average in-plane mean-squared displacements (MSDs), $\langle r(t)^2 \rangle$, over a range of time intervals t (Figure 5C). The visualized MSDs show that the lipid dynamics are subdiffusive, i.e., $\langle r(t)^2 \rangle \simeq D_\alpha t^\alpha$ with the anomalous translational diffusion coefficient D_α and the anomalous diffusion exponent $0 < \alpha < 1$.[110-111] Furthermore, a transition in the slope of the log-log MSD profiles can be observed at t ~1 ns, dividing the lipid dynamics into two distinct time regimes, which has been reported before for lipid bilayers.[112] In particular, at short times (t < 1 ns) there is little difference in the MSDs between the membranes with different carotenoid concentrations (D_α = 3.8 Å^2/ns$^\alpha$ and α = 0.6 for all membrane systems), indicating that carotenoids do not have a significant effect on the localized lipid motion. However, over longer time intervals (t > 1 ns), a change in the MSD slope is visible with changing carotenoid concentrations, suggesting that carotenoids impact larger in-plane lipid displacements. The values of D_α for 10 ns < t < 50 ns show that the presence of carotenoids reduces the dynamics of lipids, which is in line with previous reports on lipid diffusion in crowded membranes,[113-114] and that, interestingly, β-carotene seems to have a stronger effect than zeaxanthin (Figure 5D). The reduction of lipid mobility is consistent with the increase in membrane rigidity as a function of carotenoid concentration.

The membrane stiffening and condensing effects of carotenoids described in Figures 2-5 are very reminiscent of the well-studied impact of cholesterol on lipid bilayers.[12, 108, 115] Sterol molecules cause structural condensation by cohesive interactions with other lipids in the membrane and promote phase separation.[11] Cholesterol, in particular, has been shown to reduce the lateral area and enhance the order in lipid

bilayers,[116] thus it occurs predominantly in ordered rather than in disordered membrane phases.[117] The current results show that carotenoids have similar effects on POPC membranes, indicating that they could act as a substitute for cholesterol and might contribute to the formation of functional domains in lipid membranes.

β-carotene rotation and zeaxanthin H-bonding have a localized impact on the membrane structure

Despite the same trend with increasing carotenoid concentration, a slight difference is observed in the extent of membrane thickening upon adding large amounts (i.e., 5 or 10 mol%) of β-carotene compared to zeaxanthin (Figure 2 A-C). Structurally, the two carotenoids differ by the presence of two hydroxyl groups at both ends of zeaxanthin, that are absent in β-carotene (see Figure 1). Previously, umbrella sampling studies on single membrane-embedded carotenoids concluded that β-carotene could freely rotate within the membrane whereas zeaxanthin preferably remains tilted with respect to the membrane normal axis as a result of its capability to hydrogen bond (or H-bond) to lipid head groups.[65-66]

To analyze the degree of carotenoid rotation at different concentrations, we derived the population histogram of their rotation angle, Θ (Figure 6). The distribution reveals that β-carotene can even flip around the membrane midplane, i.e., rotate by up to 180°, during the (unbiased) 500 ns simulations at any concentration (Figure 6A). However, it must be noted that these rotation angle distributions are averaged over the number of carotenoids present in each system. Therefore, they do not provide information on the absolute numbers of flipped carotenoids in each system. In fact, during the entire simulations, a

total of two out of four β-carotenes (50%) flipped at 1 mol%, only one out of ten (10%) at 2.5 mol%, three out of twenty (15%) at 5 mol%, and two out of forty (5%) at 10 mol%. This indicates that β-carotene becomes less mobile at increasing concentrations, which is consistent with the increased membrane rigidity (Figure 5).

In stark contrast, zeaxanthin molecules do not flip. Instead they mostly assume a slightly tilted orientation with respect to the bilayer normal at any concentration (Figure 6B). The average value for the zeaxanthin rotation angle of ~30º agrees with previously reported results.[65-66, 118]

The flipping of β-carotene around the membrane midplane can impact the membrane structure because it affects its surrounding lipids in both leaflets at the same time. We investigated this in greater detail by calculating the tilt of POPC molecules surrounding β-carotenes (i.e., within 4 Å of their ionone rings) at any concentration. Figure 7A shows the corresponding POPC tilt distributions for different rotation angles of the nearby β-carotene molecule and Figures 7B-D visualize representative snapshots (due to the symmetry in flipping rotations, the carotenoid rotation is only given up to 90°). The lipids are most distorted when β-carotene is rotated roughly half-way between the vertical (parallel to bilayer normal) and the horizontal (perpendicular to bilayer normal) orientation, i.e., when $30° < \Theta < 60°$ (Figure 7C). The surrounding lipids are somewhat less tilted (Figure 7D) when β-carotene is about horizontal, i.e., $60° < \Theta < 90°$, and they are least affected when the nearby carotenoid assumes a vertical orientation almost parallel to the lipids, i.e., $0° < \Theta < 30°$ (Figure 7B). This reveals that the flipping of β-carotene, which is more likely at lower concentrations, can lead to simultaneous distortions in both leaflets of

the bilayer that influence the tilt and splay angles of nearby lipids and thus, as discussed above, can contribute to localized membrane undulations.

Unlike β-carotene, zeaxanthin can form H-bonds with the lipid head group oxygen atoms. These fall into 4 categories (Figure 8A): the ester phosphate oxygens (O11, O12), the non-ester phosphate oxygens (O13, O14), the acyl-chain ether oxygens (O21, O31), and the acyl-chain carbonyl oxygens (O22, O32). Figure 8B shows zeaxanthin H-bond occupancies with the POPC oxygens, P_{HB}, which is clearly the highest for the carbonyl oxygens (P_{HB} = 16.8% at 10 mol%) followed by the non-ester phosphate oxygens (P_{HB} = 5.8%). In spite of their proximity to the other oxygens, the ester phosphate oxygens (P_{HB} = 2.5%) and the ether oxygens (P_{HB} = 0.4%) only sporadically form H-bonds with zeaxanthin. This trend holds at every zeaxanthin concentration, which implicates that, regardless of their amount, about one quarter of all the zeaxanthin molecules are on average H-bonded to surrounding lipids. This value is comparable with the H-bond occupancy for a single zeaxanthin molecule in a DMPC lipid membrane reported before by Grudzinski et al. (P_{HB} = ~29% at a zeaxanthin rotation angle of 30º).[66]

To verify the importance of the lipid carbonyl oxygens for the formation of H-bonds, we simulated 10 mol% zeaxanthin in a bilayer of the ether lipid di-palmitoyl-phosphatidylcholine that lacks the carbonyl oxygens and is ubiquitous in cell membranes of mammals and bacteria. In the absence of the carbonyl oxygens, P_{HB} for both the non-ester phosphate oxygens (~7.5%, see Figure 8B) and the ether oxygens (~5.1%) is increased by ~2% and ~4%, respectively. Overall, zeaxanthin still forms fewer H-Bonds with the ether lipid (~15%) than it does with POPC (~25%).

Simultaneous H-bonding of lipids in both leaflets with the same zeaxanthin molecule may be responsible for the thinner membranes at high concentrations of zeaxanthin compared to β-carotene (see Figure 2A). On average, ~7% of all zeaxanthin molecules form such H-bonds on both ends at the same time, thus connecting the two sides of the membrane and "holding" them together. This average percentage is independent of the zeaxanthin concentration, which means that, for instance, at 10 mol%, ~3 out of 40 zeaxanthins are on average involved in coupling the two leaflets at any time. Accordingly, the percentage of leaflet-coupling H-bonds in the ether lipid bilayer is ~2.5%, corresponding to one out of 40 zeaxanthin molecules forming simultaneous H-bonds.

Although only a fraction of all the lipids are simultaneously linked through H-bonds with zeaxanthin across both leaflets, the average separation of their choline heavy atoms, which is used for the bilayer thickness calculations, is reduced (40.8 +/- 0.2 Å at 10 mol%) compared to the overall average values at the same concentration (i.e., D_B = 42.6 +/- 0.1 Å). Notably, the average tilt angle of H-bond-coupled lipids in opposite leaflets ($\delta = 20.8°$ at 10 mol%) agrees with the corresponding bulk average ($\delta = 20.2°$) of all lipids. This shows how leaflet-coupling by zeaxanthin can indeed have a localized thinning effect on the membrane structure. Figure 9 shows a representative snapshot of one zeaxanthin forming H-bonds on both ends (one with a POPC non-ester phosphate oxygen in the top leaflet and one with a POPC carbonyl oxygen in the bottom leaflet).

In general, the results on carotenoid rotation and H-bonding are consistent with previous studies in terms of average rotation angles and H-bond occupancies. However, the current simulations with variable carotenoid concentrations also reveal two previously unknown properties. First, β-carotene rotations, that can lead to localized distortions in the

lipid orientation and thus a less rigid membrane structure, are more prevalent at lower concentrations. Second, ~25% of zeaxanthin molecules form H-bonds with the lipid head group at any concentration and, in particular, ~7% of zeaxanthin molecules connect the membrane leaflets through simultaneous H-bonding of lipids on opposite sides. Both of these effects, i.e., the reduction of β-carotene rotations and the higher count of zeaxanthin H-bonds at high carotenoid concentrations, can contribute to the slight difference in the extent of membrane condensation between the two carotenoids observed at these concentrations.

Conclusion

Small molecules can have strong effects on biomembrane structure and function through direct interactions with the lipid components.[4, 12, 14] In this regard, carotenoids are an intriguing example of natural membrane additives because they usually span both bilayer leaflets, allowing them to interact with the lipids on both sides simultaneously.

The present simulation results show that both β-carotene and zeaxanthin have a condensing effect on the POPC lipid bilayer that is similar to that of cholesterol, i.e., individual lipids are more tightly packed, as in the presence of sterols. Consequently, the membrane becomes thicker and more rigid the more carotenoids it contains. Although the membrane with 10 mol% of either carotenoid is predicted to be somewhat less rigid than that with the same amount of cholesterol, the current study reveals that carotenoids have effects similar to sterols on model biomembranes.

Sterols regulate the membrane fluid phase behavior and are predominantly associated with a liquid-ordered membrane phase. Cholesterol in animals, ergosterol in

fungi, and stigmasterol and sitosterol in plants are all involved in the formation of lipid raft domains that maintain unique composition, structure and dynamics in the cell membrane.[19] Hopanoids are a different class of polycyclic terpenoids that occur in bacteria and have been reported to promote phase separation in lipid vesicles.[119] Hopanoids are structurally related to the sterols, as they share the same noncyclic polyisoprenoid precursor molecule, squalene. Carotenoids are also noncyclic polyisoprenoid molecules, that occur in bacterial cell membranes and have recently been suggested to contribute to the formation of functional membrane microdomains.[40-42] It is conceivable that all the above-mentioned structurally related membrane components share a functional relationship, too. The results of the current study substantiate the hypothesis that carotenoids act as a surrogate for cholesterol in the formation of functional membrane domains.

In this context, it should be noted that cholesterol is essentially a bidirectional regulator of membrane fluidity. Although, at biologically relevant temperatures, it stabilizes membranes, at low temperatures cholesterol can interfere with the packing of phospholipids, thus increasing the membrane fluidity.[12] Whether different carotenoids have a similar effect on membranes at low temperature is beyond the scope of this study, but it is worth exploring in the future in order to gain a fuller understanding of how carotenoids exert their effects on membranes.

β-carotene and zeaxanthin differ structurally by the presence of a single hydroxyl group on both ends of the latter carotenoid. Previous experiments have reported that this small structural difference can actually lead to fairly different orientations of the two carotenoids in lipid membranes.[38] In fact, in previous simulations, we have shown that they modulate the liquid ordered and disordered phases of lipid membranes through different

mechanisms.[67] Interestingly, in both phases, carotenoids (at a concentration of 10 mol%) were shown to lead to a vertical compression of the membrane, i.e., an opposite effect to the lateral condensation of POPC membranes reported in the current study. However, those simulations of the ordered and disordered phases were performed on membranes that are less fluid than a pure POPC membrane[120] as they also contained a high-melting phospholipid (1,2-distearoyl-sn-glycero-3-phosphocholine) plus cholesterol. Thus, it is not surprising that carotenoids show a different effect on the more fluid POPC-only membrane in this study.

The current simulations confirm that the carotenoids can assume different orientations in a lipid bilayer and the results further suggest that the presence or absence of the hydroxyl groups entails localized effects on the membrane structure, as rotating β-carotenes can locally distort the lipid orientations and H-bonding zeaxanthins can hold the membrane leaflets together. These effects may be responsible for the slightly stronger condensation effect of β-carotene compared to zeaxanthin at high concentrations.

In spite of the different interactions with the lipid molecules, both carotenoids are essentially accommodated in the lipid membrane by tilting (and kinking their ionone rings on both ends) and simultaneously expanding the bilayer to some extent. The degree to which these interacting effects unfold depends on the identity and the abundance of all membrane components, i.e., all lipid and carotenoid types. This study has revealed that membranes formed purely by POPC, a lipid with one unsaturated acyl chain, are condensed by β-carotene and zeaxanthin to different degrees at different concentrations. Nevertheless, it is conceivable that these two carotenoids will likely have slightly different effects on the lateral packing and condensation of different membranes, for example, a small

condensation effect on bilayers that consist of lipids with fully saturated acyl chains, such as DMPC or DPPC. In order to test if carotenoids are indeed suitable sterol substitutes for the formation of functional microdomains in bacterial membranes, future studies should incorporate more bacterial membrane components, i.e., lipids with different head groups and differently branched acyl chains[121-122] as well as hopanoids and different amounts of carotenoids.

Acknowledgements

We would like to thank Dr. Javier Cerezo for providing the carotenoid parameters that were used in this work. This research was partially supported by an ASCR Leadership Computing Challenge (ALCC) award and used the resources of the Oak Ridge Leadership Computing Facility at the Oak Ridge National Laboratory, which is supported by the Office of Science of the U.S. Department of Energy under Contract No. DE-AC05-00OR22725. This research also used resources of the National Energy Research Scientific Computing Center, a DOE Office of Science User Facility supported by the Office of Science of the U.S. Department of Energy under Contract No. DE-AC02- 05CH11231. JCS acknowledges support from U.S D.O.E. B.E.R. Contract FWP ERKP752.

References

1. Gennis, R., *Biomembranes: Molecular Structure and Function*. Springer: 1988.
2. Murate, M.; Kobayashi, T., Revisiting transbilayer distribution of lipids in the plasma membrane. *Chemistry and Physics of Lipids* **2016,** *194*, 58-71.
3. Forrest, L., Structural Symmetry in Membrane Proteins. *Annual Review of Biophysics* **2015,** *44* (1), 311-337.

4. Meerschaert, R.; Kelly, C., Trace membrane additives affect lipid phases with distinct mechanisms: a modified Ising model. *European biophysics journal : EBJ* **2015,** *44* (4), 227-233.
5. Koldsø, H.; Shorthouse, D.; Hélie, J.; Sansom, M., Lipid clustering correlates with membrane curvature as revealed by molecular simulations of complex lipid bilayers. *PLoS computational biology* **2014,** *10* (10).
6. van Meer, G.; Voelker, D.; Feigenson, G., Membrane lipids: where they are and how they behave. *Nature Reviews Molecular Cell Biology* **2008,** *9* (2), 112-124.
7. Sodt, A.; Sandar, M.; Gawrisch, K.; Pastor, R.; Lyman, E., The Molecular Structure of the Liquid-Ordered Phase of Lipid Bilayers. *J. Am. Chem. Soc.* **2014,** *136* (2), 725-732.
8. Cheng, X.; Smith, J., Biological Membrane Organization and Cellular Signaling. *Chemical Reviews* **2019,** *119*, 5849-5880.
9. Lingwood, D.; Simons, K., Lipid Rafts As a Membrane-Organizing Principle. *Science* **2010,** *327* (5961), 46-50.
10. Ribeiro, N.; Streiff, S.; Heissler, D.; Elhabiri, M.; Albrecht-Gary, A. M.; Atsumi, M.; Gotoh, M.; Desaubry, L.; Nakatani, Y.; Ourisson, G., Reinforcing effect of bi- and tri-cyclopolyprenols on 'primitive' membranes made of polyprenyl phosphates. *Tetrahedron* **2007,** *63* (16), 3395-3407.
11. Dufourc, E. J., Sterols and Membrane Dynamics. *Journal of Chemical Biology* **2008,** *1*, 63-77.
12. de Meyer, F.; Smit, B., Effect of cholesterol on the structure of a phospholipid bilayer. *Proceedings of the National Academy of Sciences of the United States of America* **2009,** *106* (10), 3654-3658.
13. Hsieh, C.-J.; Chen, Y.-W.; Hwang, D., Effects of cholesterol on membrane molecular dynamics studied by fast field cycling NMR relaxometry. *Phys. Chem. Chem. Phys.* **2013,** *15* (39), 16634-16640.
14. Khelashvili, G.; Johner, N.; Zhao, G.; Harries, D.; Scott, H. L., Molecular origins of bending rigidity in lipids with isolated and conjugated double bonds: The effect of cholesterol. *Chemistry and Physics of Lipids* **2014,** *178*, 18-26.
15. Yang, S.-T.; Kreutzberger, A. J. B.; Lee, J.; Kiessling, V.; Tamm, L. K., The Role of Cholesterol in Membrane Fusion. *Chemistry and Physics of Lipids* **2016,** *199*, 136-143.
16. Gimpl, G.; Reitz, J.; Brauer, S.; Trossen, C., Oxytocin receptors: ligand binding, signalling and cholesterol dependence. *Progress in Brain Research* **2008,** *170*, 193-204.
17. Saxena, R.; Chattopadhyay, A., Membrane cholesterol stabilizes the human serotonin(1A) receptor. *Biochimica et Biophysica Acta (BBA) - Biomembranes* **2012,** *1818* (12), 2936-2942.
18. Elson, E. L.; Fried, E.; Dolbow, J. E.; Genin, G. M., Phase separation in biological membranes: integration of theory and experiment. *Annual review of biophysics* **2010,** *39*, 207-226.
19. Song, Y.; Kenworthy, A. K.; Sanders, C. R., Cholesterol as a co-solvent and a ligand for membrane proteins. *Protein Science* **2014,** *23*, 1-22.
20. Gruszecki, W., Carotenoids in Membranes. In *The Photochemistry of Carotenoids*, Frank, H.; Young, A.; Britton, G.; Cogdell, R., Eds. Springer Netherlands: 1999; Vol. 8, pp 363-379.

21. Havaux, M., Carotenoids as membrane stabilizers in chloroplasts. *Trends in Plant Science* **1998,** *3* (4), 147-151.
22. Cogdell, R.; Gardiner, A., Functions of carotenoids in photosynthesis. *Methods in Enzymology* **1993,** *214*, 185-193.
23. Trebst, A., Function of beta-carotene and tocopherol in photosystem II. *Zeitschrift fur Naturforschung. C, Journal of biosciences* **2003,** *58* (9-10), 609-620.
24. Hashimoto, H.; Uragami, C.; Cogdell, R., Carotenoids and Photosynthesis. *Sub-cellular biochemistry* **2016,** *79*, 111-139.
25. Liguori, N.; Xu, P.; van Stokkum, I. H. M.; van Oort, B.; Lu, Y.; Karcher, D.; Bock, R.; Croce, R., Different carotenoid conformations have distinct functions in light-harvesting regulation in plants. *Nature Communications* **2017,** *8*, 1994.
26. Frank, H.; Bautista, J.; Josue, J.; Young, A., Mechanism of Nonphotochemical Quenching in Green Plants: Energies of the Lowest Excited Singlet States of Violaxanthin and Zeaxanthin. *Biochemistry* **2000,** *39* (11), 2831-2837.
27. Miller, N.; Sampson, J.; Candeias, L.; Bramley, P.; Rice-Evans, C., Antioxidant activities of carotenes and xanthophylls. *FEBS Letters* **1996,** *384* (3), 240-242.
28. Britton, G., Structure and properties of carotenoids in relation to function. *FASEB journal* **1995,** *9* (15), 1551-1558.
29. Bernstein, P. S.; Khachik, F.; Carvalho, L. S.; Muir, G. J.; Zhao, D. Y.; Katz, N. B., Identification and quantitation of carotenoids and their metabolites in the tissues of the human eye. *Experimental eye research* **2001,** *72* (3), 215-223.
30. Landrum, J. T.; Bone, R. A., Lutein, zeaxanthin, and the macular pigment. *Archives of biochemistry and biophysics* **2001,** *385* (1), 28-40.
31. Dowling, D.; Simmons, L., Reactive oxygen species as universal constraints in life-history evolution. *Proceedings of the Royal Society of London B: Biological Sciences* **2009,** *276* (1663), 1737-1745.
32. Mayne, S. T., Beta-carotene, carotenoids, and disease prevention in humans. *FASEB journal* **1996,** *10* (7), 690-701.
33. Stahl, W.; Sies, H., Antioxidant Defense: Vitamins E and C and Carotenoids. *Diabetes* **1997,** *46* (Supplement 2), S14-S18.
34. Johnson, E., The role of carotenoids in human health. *Nutrition in clinical care : an official publication of Tufts University* **2002,** *5* (2), 56-65.
35. Stahl, W.; Sies, H., Bioactivity and protective effects of natural carotenoids. *Biochimica et Biophysica Acta (BBA) - Molecular Basis of Disease* **2005,** *1740* (2), 101-107.
36. Kidd, P., Astaxanthin, cell membrane nutrient with diverse clinical benefits and anti-aging potential. *Alternative medicine review : a journal of clinical therapeutic* **2011,** *16* (4), 355-364.
37. Voutilainen, S.; Nurmi, T.; Mursu, J.; Rissanen, T., Carotenoids and cardiovascular health. *The American Journal of Clinical Nutrition* **2006,** *83* (6), 1265-1271.
38. Gruszecki, W.; Strzałka, K., Carotenoids as modulators of lipid membrane physical properties. *Biochimica et biophysica acta* **2005,** *1740* (2), 108-115.
39. McNulty, H.; Byun, J.; Lockwood, S.; Jacob, R.; Mason, P., Differential effects of carotenoids on lipid peroxidation due to membrane interactions: X-ray diffraction analysis. *Biochimica et biophysica acta* **2007,** *1768* (1), 167-174.

40. Lopez, D.; Kolter, R., Functional microdomains in bacterial membranes. *Genes & Development* **2010,** *24*, 1893-1902.
41. Bramkamp, M.; Lopez, D., Exploring the Existence of Lipid Rafts in Bacteria. *Microbiology and Molecular Biology Reviews* **2015,** *79*, 81-100.
42. Lopez, D.; Koch, G., Exploring functional membrane microdomains in bacteria: an overview. *Current Opinion in Microbiology* **2017,** *36*, 76-84.
43. Garcia-Fernandez, E.; Koch, G.; Wagner, R. M.; Fekete, A.; Stengel, S. T.; Schneider, J.; Mielich-Suess, B.; Geibel, S.; Markert, S. M.; Stigloher, C.; Lopez, D., Membrane Microdomain Disassembly Inhibits MRSA Antibiotic Resistance. *Cell* **2017,** *171* (6), 1354-1367.
44. Gruszecki, W. I.; Sielewiesiuk, J., Galactolipid multibilayers modified with xanthophylls: orientational and diffractometric studies. *Biochimica et biophysica acta* **1991,** *1069* (1), 21-26.
45. Sujak, A.; Mazurek, P.; Gruszecki, W., Xanthophyll pigments lutein and zeaxanthin in lipid multibilayers formed with dimyristoylphosphatidylcholine. *Journal of photochemistry and photobiology. B, Biology* **2002,** *68* (1), 39-44.
46. Suwalsky, M.; Hidalgo, P.; Strzalka, K.; Kostecka-Gugala, A., Comparative X-ray studies on the interaction of carotenoids with a model phosphatidylcholine membrane. *Zeitschrift fur Naturforschung. C, Journal of biosciences* **2002,** *57* (1-2), 129-134.
47. Subczynski, W.; Markowska, E.; Sielewiesiuk, J., Effect of polar carotenoids on the oxygen diffusion-concentration product in lipid bilayers. An EPR spin label study. *Biochimica et Biophysica Acta (BBA) - Biomembranes* **1991,** *1068* (1), 68-72.
48. Jezowska, I.; Wolak, A.; Gruszecki, W. I.; Strzałka, K., Effect of beta-carotene on structural and dynamic properties of model phosphatidylcholine membranes. II. A 31P-NMR and 13C-NMR study. *Biochimica et biophysica acta* **1994,** *1194* (1), 143-148.
49. Gabrielska, J.; Gruszecki, W. I., Zeaxanthin (dihydroxy-beta-carotene) but not beta-carotene rigidifies lipid membranes: a 1H-NMR study of carotenoid-egg phosphatidylcholine liposomes. *Biochimica et biophysica acta* **1996,** *1285* (2), 167-174.
50. Berglund, A.; Nilsson, R.; Liljenberg, C., Permeability of large unilamellar digalactosyldiacylglycerol vesicles for protons and glucose – influence of α-tocopherol, β-carotene, zeaxanthin and cholesterol. *Plant Physiology and Biochemistry* **1999,** *37* (3), 179-186.
51. Ingólfsson, H.; Melo, M.; van Eerden, F.; Arnarez, C.; Lopez, C.; Wassenaar, T.; Periole, X.; de Vries, A.; Tieleman, P.; Marrink, S., Lipid Organization of the Plasma Membrane. *J. Am. Chem. Soc.* **2014,** *136* (41), 14554-14559.
52. Bennett, D.; Tieleman, P., Computer simulations of lipid membrane domains. *Biochimica et Biophysica Acta (BBA) - Biomembranes* **2013,** *1828* (8), 1765-1776.
53. Hong, C.; Tieleman, P.; Wang, Y., Microsecond Molecular Dynamics Simulations of Lipid Mixing. *Langmuir* **2014,** *30* (40), 11993-12001.
54. Ackerman, D.; Feigenson, G., Multiscale Modeling of Four-Component Lipid Mixtures: Domain Composition, Size, Alignment, and Properties of the Phase Interface. *J. Phys. Chem. B* **2015,** *119* (11), 4240-4250.
55. Braun, A.; Sachs, J., Determining Structural and Mechanical Properties from Molecular Dynamics Simulations of Lipid Vesicles. *J. Chem. Theory Comput.* **2014,** *10* (9), 4160-4168.

56. Perlmutter, J.; Sachs, J., Interleaflet Interaction and Asymmetry in Phase Separated Lipid Bilayers: Molecular Dynamics Simulations. *Journal of the American Chemical Society* **2011,** *133* (17), 6563-6577.
57. Tian, J.; Nickels, J.; Katsaras, J.; Cheng, X., Behavior of Bilayer Leaflets in Asymmetric Model Membranes: Atomistic Simulation Studies. *J. Phys. Chem. B* **2016,** *120* (33), 8438-8448.
58. Nickels, J.; Smith, J.; Cheng, X., Lateral organization, bilayer asymmetry, and inter-leaflet coupling of biological membranes. *Chemistry and physics of lipids* **2015,** *192*, 87-99.
59. Hofsäss, C.; Lindahl, E.; Edholm, O., Molecular dynamics simulations of phospholipid bilayers with cholesterol. *Biophysical journal* **2003,** *84* (4), 2192-2206.
60. Berkowitz, M. L., Detailed molecular dynamics simulations of model biological membranes containing cholesterol. *Biochimica et Biophysica Acta - Biomembranes* **2009,** *1788* (1), 86-96.
61. Zhao, G.; Subbaiah, P. V.; Mintzer, E.; Chiu, S. W.; Jakobsson, E.; Scott, H. L., Molecular dynamic simulation study of cholesterol and conjugated double bonds in lipid bilayers. *Chemistry and Physics of Lipids* **2011,** *164* (8), 811-818.
62. MacDermaid, C.; Kashyap, H.; DeVane, R.; Shinoda, W.; Klauda, J.; Klein, M.; Fiorin, G., Molecular dynamics simulations of cholesterol-rich membranes using a coarse-grained force field for cyclic alkanes. *The Journal of chemical physics* **2015,** *143* (24).
63. Vogel, A.; Scheidt, H.; Baek, D.; Bittman, R.; Huster, D., Structure and dynamics of the aliphatic cholesterol side chain in membranes as studied by 2H NMR spectroscopy and molecular dynamics simulation. *Phys. Chem. Chem. Phys.* **2016,** *18* (5), 3730-3738.
64. Jemiola-Rzeminska, M.; Pasenkiewicz-Gierula, M.; Strzalka, K., The behaviour of β-carotene in the phosphatidylcholine bilayer as revealed by a molecular simulation study. *Chemistry and Physics of Lipids* **2005,** *135*, 27-37.
65. Cerezo, J.; Zúñiga, J.; Bastida, A.; Requena, A.; José, P., Conformational changes of β-carotene and zeaxanthin immersed in a model membrane through atomistic molecular dynamics simulations. *Physical chemistry chemical physics : PCCP* **2013,** *15* (17), 6527-6538.
66. Grudzinski, W.; Nierzwicki, L.; Welc, R.; Reszczynska, E.; Luchowski, R.; Czub, J.; Gruszecki, W. I., Localization and Orientation of Xanthophylls in a Lipid Bilayer. *Scientific Reports* **2017,** *7*.
67. Johnson, Q.; Mostofian, B.; Fuente Gomez, G.; Smith, J.; Cheng, X., Effects of carotenoids on lipid bilayers. *Phys. Chem. Chem. Phys.* **2018,** *20* (5), 3795-3804.
68. Shityakov, S.; Dandekar, T., Molecular Dynamics Simulation of Popc and Pope Lipid Membrane Bilayers Enforced by an Intercalated Single-Wall Carbon Nanotube. *Nano Brief Reports and Reviews* **2011,** *6* (1), 19-29.
69. Wang, H.; Ren, X.; Meng, F., Molecular dynamics simulation of six β-blocker drugs passing across POPC bilayer. *Molecular Simulation* **2016,** *42* (1), 56-63.
70. Zhao, L.; Cao, Z.; Bian, Y.; Hu, G.; Wang, J.; Zhou, Y., Molecular Dynamics Simulations of Human Antimicrobial Peptide LL-37 in Model POPC and POPG Lipid Bilayers. *International journal of molecular sciences* **2018,** *19* (4).

71. Widomska, J.; Zareba, M.; Subczynski, W. K., Can Xanthophyll-Membrane Interactions Explain Their Selective Presence in the Retina and Brain? *Foods (Basel, Switzerland)* **2016,** *5* (1).
72. Martínez, L.; Andrade, R.; Birgin, E. G.; Martínez, J. M., PACKMOL: a package for building initial configurations for molecular dynamics simulations. *Journal of computational chemistry* **2009,** *30* (13), 2157-2164.
73. Jorgensen, W.; Chandrasekhar, J.; Madura, J.; Impey, R.; Klein, M., Comparison of simple potential functions for simulating liquid water. *The Journal of Chemical Physics* **1983,** *79* (2), 926-935.
74. Klauda, J.; Venable, R.; Freites, A.; O'Connor, J.; Tobias, D.; Mondragon-Ramirez, C.; Vorobyov, I.; MacKerell, A.; Pastor, R., Update of the CHARMM all-atom additive force field for lipids: validation on six lipid types. *The Journal of Physical Chemistry B* **2010,** *114* (23), 7830-7843.
75. Pastor, R. W.; Mackerell, A. D., Development of the CHARMM Force Field for Lipids. *The journal of physical chemistry letters* **2011,** *2* (13), 1526-1532.
76. Pan, J.; Cheng, X.; Heberle, F.; Mostofian, B.; Kučerka, N.; Drazba, P.; Katsaras, J., Interactions between Ether Phospholipids and Cholesterol As Determined by Scattering and Molecular Dynamics Simulations. *The Journal of Physical Chemistry B* **2012,** *116* (51), 14829-14838.
77. Martyna, G. J.; Tobias, D. J.; Klein, M. L., Constant pressure molecular dynamics algorithms. *The Journal of Chemical Physics* **1994,** *101* (5), 4177-4189.
78. Pastor, R. W.; Brooks, B. R.; Szabo, A., An analysis of the accuracy of Langevin and molecular dynamics algorithms. *Molecular Physics* **1988,** *65* (6), 1409-1419.
79. Feller, S. E.; Zhang, Y.; Pastor, R. W., Constant pressure molecular dynamics simulation: The Langevin piston method. *The Journal of Chemical Physics* **1995,** *103*, 4613-4621.
80. Darden, T.; York, D.; Pedersen, L., Particle mesh Ewald: An N·log(N) method for Ewald sums in large systems. *The Journal of Chemical Physics* **1993,** *98* (12), 10089-10092.
81. Essmann, U.; Perera, L.; Berkowitz, M.; Darden, T.; Lee, H.; Pedersen, L., A smooth particle mesh Ewald method. *The Journal of Chemical Physics* **1995,** *103* (19), 8577-8593.
82. Ryckaert, J.-p.; Ciccotti, G.; Berendsen, H. In *Numerical integration of the Cartesian equations of motion of a system with constraints: molecular dynamics of n-alkanes*, J. Comput. Phys, 1977; pp 327-341.
83. Phillips, J.; Braun, R.; Wang, W.; Gumbart, J.; Tajkhorshid, E.; Villa, E.; Chipot, C.; Skeel, R.; Kalé, L.; Schulten, K., Scalable molecular dynamics with NAMD. *Journal of computational chemistry* **2005,** *26* (16), 1781-1802.
84. Piggot, T.; Allison, J.; Sessions, R.; Essex, J., On the Calculation of Acyl Chain Order Parameters from Lipid Simulations. *Journal of chemical theory and computation* **2017,** *13* (11), 5683-5696.
85. Khelashvili, G.; Kollmitzer, B.; Heftberger, P.; Pabst, G.; Harries, D., Calculating the Bending Modulus for Multicomponent Lipid Membranes in Different Thermodynamic Phases. *Journal of Chemical Theory and Computation* **2013,** *9* (9), 3866-3871.

86. Reddy, T. diffusion_analysis_MD_simulations: Initial Release (Version 1.0). Zenodo. http://doi.org/10.5281/zenodo.11827.
87. Reddy, T.; Sansom, M. S. P., The Role of the Membrane in the Structure and Biophysical Robustness of the Dengue Virion Envelope. *Structure* **2016,** *24* (3), 375-382.
88. Mostofian, B.; Zuckerman, D. M., Statistical Uncertainty Analysis for Small-Sample, High Log-Variance Data: Cautions for Bootstrapping and Bayesian Bootstrapping. *Journal of chemical theory and computation* **2019,** *15* (6), 3499-3509.
89. Humphrey, W.; Dalke, A.; Schulten, K., VMD: visual molecular dynamics. *Journal of molecular graphics* **1996,** *14* (1).
90. Kucerka, N.; Nagle, J.; Sachs, J.; Feller, S.; Pencer, J.; Jackson, A.; Katsaras, J., Lipid bilayer structure determined by the simultaneous analysis of neutron and X-ray scattering data. *Biophysical journal* **2008,** *95* (5), 2356-2367.
91. Kučerka, N.; Nieh, M.-P.; Katsaras, J., Fluid phase lipid areas and bilayer thicknesses of commonly used phosphatidylcholines as a function of temperature. *Biochimica et biophysica acta* **2011,** *1808* (11), 2761-2771.
92. Smaby, J. M.; Momsen, M. M.; Brockman, H. L.; Brown, R. E., Phosphatidylcholine Acyl Unsaturation Modulates the Decrease in Interfacial Elasticity Induced by Cholesterol. *Biophysical Journal* **1997,** *73*, 1492-1505.
93. Hodzic, A.; Zoumpoulakis, P.; Pabst, G.; Mavromoustakos, T.; Rappolt, M., Losartan's affinity to fluid bilayers modulates lipid–cholesterol interactions *Physical chemistry chemical physics* **2012,** *14*, 4780-4788.
94. Daily, M. D.; Olsen, B. N.; Schlesinger, P. H.; Ory, D. S.; Baker, N. A., Improved Coarse-Grained Modeling of Cholesterol-Containing Lipid Bilayers. *Journal of chemical theory and computation* **2014,** *10* (5), 2137-2150.
95. Williamson, J.; Olmsted, P., Registered and antiregistered phase separation of mixed amphiphilic bilayers. *Biophysical journal* **2015,** *108* (8), 1963-1976.
96. Bleecker, J.; Cox, P.; Foster, R.; Litz, J.; Blosser, M.; Castner, D.; Keller, S., Thickness Mismatch of Coexisting Liquid Phases in Noncanonical Lipid Bilayers. *The journal of physical chemistry. B* **2016,** *120* (10), 2761-2770.
97. Fowler, P.; Williamson, J.; Sansom, M.; Olmsted, P., Roles of Interleaflet Coupling and Hydrophobic Mismatch in Lipid Membrane Phase-Separation Kinetics. *Journal of the American Chemical Society* **2016,** *138* (36), 11633-11642.
98. Petrache, H. I.; Dodd, S. W.; Brown, M. F., Area per lipid and acyl length distributions in fluid phosphatidylcholines determined by (2)H NMR spectroscopy. *Biophysical journal* **2000,** *79* (6), 3172-3192.
99. Nagle, J. F.; Tristram-Nagle, S., Structure of lipid bilayers. *Biochimica et biophysica acta* **2000,** *1469* (3), 159-195.
100. Leekumjorn, S.; Sum, A. K., Molecular Simulation Study of Structural and Dynamic Properties of Mixed DPPC/DPPE Bilayers. *Biophysical Journal* **2006,** *90*, 3951-3965.
101. Seelig, A.; Seelig, J., The dynamic structure of fatty acyl chains in a phospholipid bilayer measured by deuterium magnetic resonance. *Biochemistry* **1974,** *13* (23), 4839-4845.
102. Akimov, S. A.; Kuzmin, P. I.; Zimmerberg, J.; Cohen, F. S.; Chizmadzhev, Y. A., An Elastic Theory for Line Tension at a Boundary Separating Two Lipid Monolayer

Regions of Different Thickness. *Journal of Electroanalytical Chemistry* **2004,** *564*, 13-18.
103. Cooke, I.; Deserno, M., Coupling between lipid shape and membrane curvature. *Biophysical journal* **2006,** *91* (2), 487-495.
104. Capponi, S.; Freites, A.; Tobias, D.; White, S., Interleaflet mixing and coupling in liquid-disordered phospholipid bilayers. *Biochimica et biophysica acta* **2016,** *1858* (2), 354-362.
105. Watson, M.; Brandt, E.; Welch, P.; Brown, F., Determining biomembrane bending rigidities from simulations of modest size. *Physical review letters* **2012,** *109* (2).
106. Doktorova, M.; Harries, D.; Khelashvili, G., Determination of bending rigidity and tilt modulus of lipid membranes from real-space fluctuation analysis of molecular dynamics simulations. *Physical chemistry chemical physics : PCCP* **2017,** *19* (25), 16806-16818.
107. Kinnun, J.; Mallikarjunaiah, K. J.; Petrache, H.; Brown, M., Elastic deformation and area per lipid of membranes: atomistic view from solid-state deuterium NMR spectroscopy. *Biochimica et biophysica acta* **2015,** *1848* (1 Pt B), 246-259.
108. Arriaga, L.; López-Montero, I.; Monroy, F.; Orts-Gil, G.; Farago, B.; Hellweg, T., Stiffening effect of cholesterol on disordered lipid phases: a combined neutron spin echo + dynamic light scattering analysis of the bending elasticity of large unilamellar vesicles. *Biophysical journal* **2009,** *96* (9), 3629-3637.
109. Dimova, R., Recent developments in the field of bending rigidity measurements on membranes. *Advances in Colloid and Interface Science* **2014,** *208*, 225-234.
110. Kneller, G. R.; Baczynski, K.; Pasenkiewicz-Gierula, M., Consistent Picture of Lateral Subdiffusion in Lipid Bilayers: Molecular Dynamics Simulation and Exact Results *The Journal of Chemical Physics* **2011,** *135* (14), 141105.
111. Metzler, R.; Jeon, J.-H.; Cherstvy, A. G., Non-Brownian diffusion in lipid membranes: Experiments and simulations. *Biochimica et Biophysica Acta (BBA) - Biomembranes* **2016,** *1858* (10), 2451-2467.
112. Flenner, E.; Das, J.; Rheinstädter, M. C.; Kosztin, I., Subdiffusion and lateral diffusion coefficient of lipid atoms and molecules in phospholipid bilayers. *Physical Review E* **2009,** *79* (1), 011907.
113. Jeon, J.-H.; Martinez-Seara, H.; Javanainen, M.; Metzler, R., Anomalous Diffusion of Phospholipids and Cholesterols in a Lipid Bilayer and its Origins. *Physical Review Letters* **2012,** *109* (18), 188103.
114. Duncan, A. L.; Reddy, T.; Koldsø, H.; Hélie, J.; Fowler, P.; Chavent, M.; Sansom, M. S. P., Protein crowding and lipid complexity influence the nanoscale dynamic organization of ion channels in cell membranes. *Scientific Reports* **2017,** *7*, 16647.
115. Hung, W.-C.; Lee, M.-T.; Chen, F.-Y.; Huang, H., The condensing effect of cholesterol in lipid bilayers. *Biophysical journal* **2007,** *92* (11), 3960-3967.
116. Leftin, A.; Molugu, T.; Job, C.; Beyer, K.; Brown, M., Area per lipid and cholesterol interactions in membranes from separated local-field (13)C NMR spectroscopy. *Biophysical journal* **2014,** *107* (10), 2274-2286.
117. Marsh, D., Liquid-ordered phases induced by cholesterol: a compendium of binary phase diagrams. *Biochimica et biophysica acta* **2010,** *1798* (3), 688-699.

118. Gruszecki, W. I.; Sielewiesiuk, J., Orientation of xanthophylls in phosphatidylcholine multibilayers. *Biochimica et Biophysica Acta - Biomembranes* **1990,** *1023* (3), 405-412.
119. Saenz, J. P.; Sezgin, E.; Schwille, P.; Simmons, K., Functional convergence of hopanoids and sterols in membrane ordering. *Proceedings of the National Academy of Sciences of the United States of America* **2012,** *109* (35), 14236-14240.
120. Pande, A. H.; Qin, S.; Tatulian, S. A., Membrane Fluidity Is a Key Modulator of Membrane Binding, Insertion, and Activity of 5-Lipoxygenase. *Biophysical journal* **2005,** *88* (6), 4084-4094.
121. Sohlenkamp, C.; Geiger, O., Bacterial membrane lipids: diversity in structures and pathways. *Microbiology Reviews* **2016,** *40* (1), 133-159.
122. Mostofian, B.; Zhuang, T.; Cheng, X.; Nickels, J. D., Branched-Chain Fatty Acid Content Modulates Structure, Fluidity, and Phase in Model Microbial Cell Membranes. *The Journal of Physical Chemistry B* **2019,** *123* (27), 5814-5821.

Figures

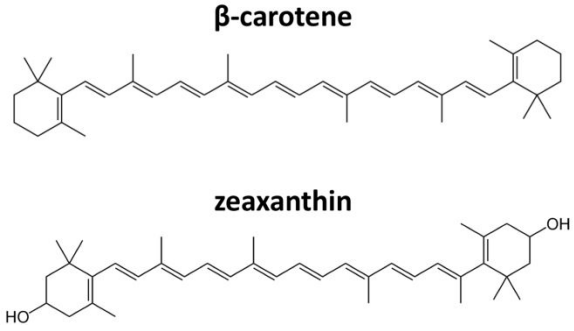

Figure 1. Molecular structures of β-carotene (top) and zeaxanthin (bottom). Both molecules have a chain of conjugated double bonds and an ionone ring structure. Zeaxanthin contains a single hydroxyl group on both ionone rings.

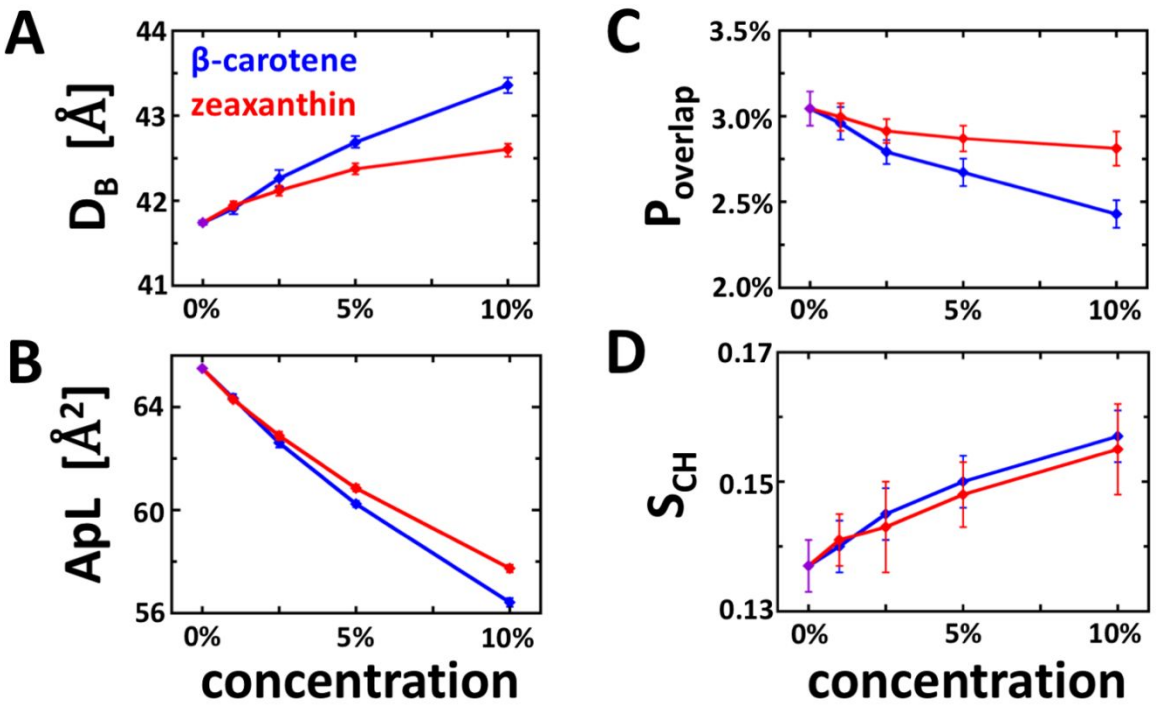

Figure 2. Membrane structural changes at different amounts of carotenoids. (a) Bilayer thickness, (b) area per lipid, (c) interdigitation of the bilayer leaflets, measured as the overlap integral of acyl chain density functions (see Figure 3C), and (d) order parameters averaged over all carbons of both acyl chains as a function of β-carotene (blue) or zeaxanthin (red) concentrations.

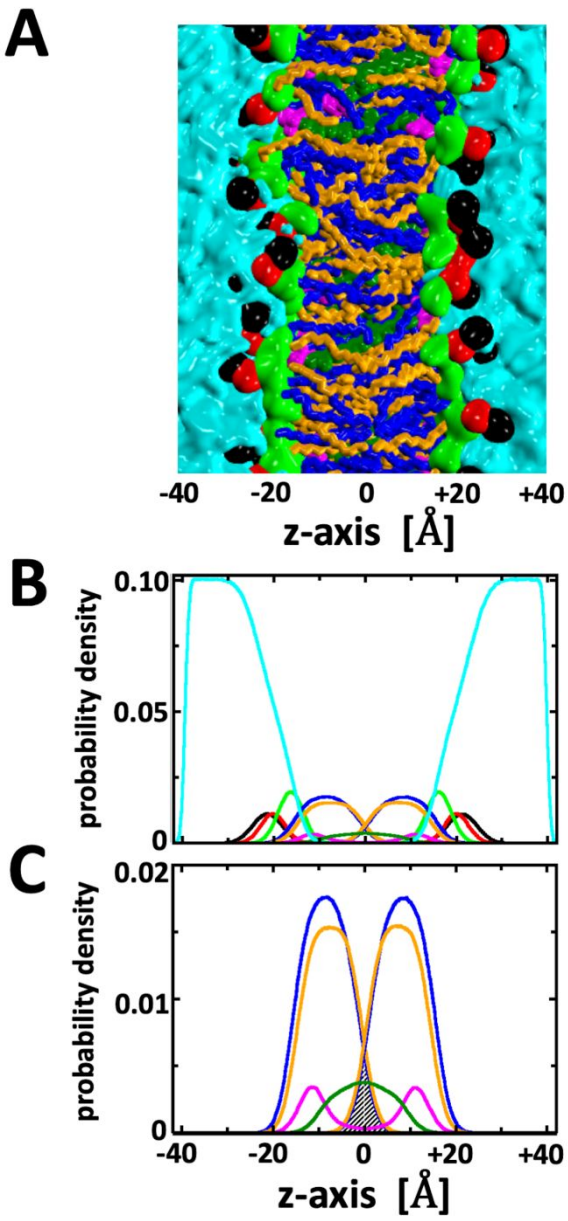

Figure 3. Densities along the membrane normal axis. (a) A space filling representation of the POPC bilayer structure with different functional groups in different colors: *sn-1* acyl chain (orange), *sn-2* acyl chain (blue), glycerol (green), phosphate (red), and choline (black). The water (cyan) and the carotenoid conjugated chain of double bonds (dark green) and ionone rings (magenta) are also visualized in different colors. The structure is a snapshot from the simulation with 10 mol% β-carotene and is shown with the membrane normal axis oriented horizontally. (b) Probability densities of different functional groups

along the bilayer normal z-axis from the simulation of 10 mol% β-carotene in a POPC bilayer. The colors correspond to those from Figure 3A. (c) Probability densities of the acyl chains and carotenoid groups along the bilayer normal z-axis (zoomed-in Figure 3B). The shaded region indicates the overlap of the opposing leaflets.

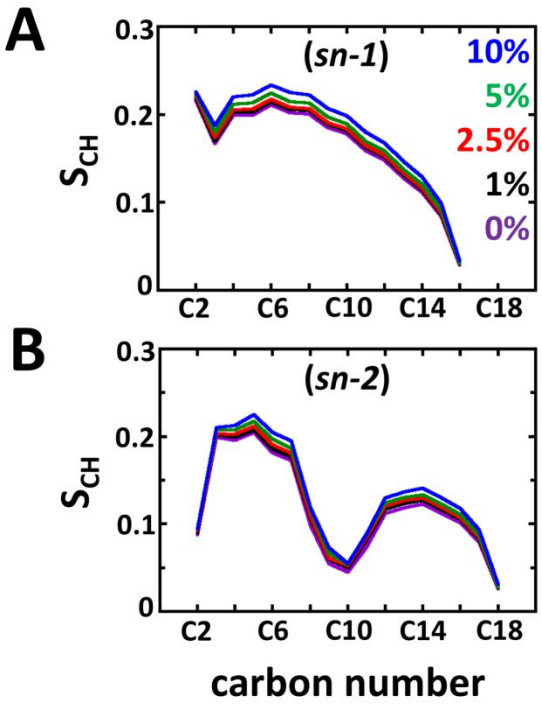

Figure 4. Lipid order parameters of (a) all 16 carbon atoms along the *sn-1* acyl chain and (b) all 18 carbon atoms along the *sn*-2 acyl chain at different concentrations of β-carotene. Note a drop in the order parameter at the C9=C10 double bond in the *sn-2* acyl chain.

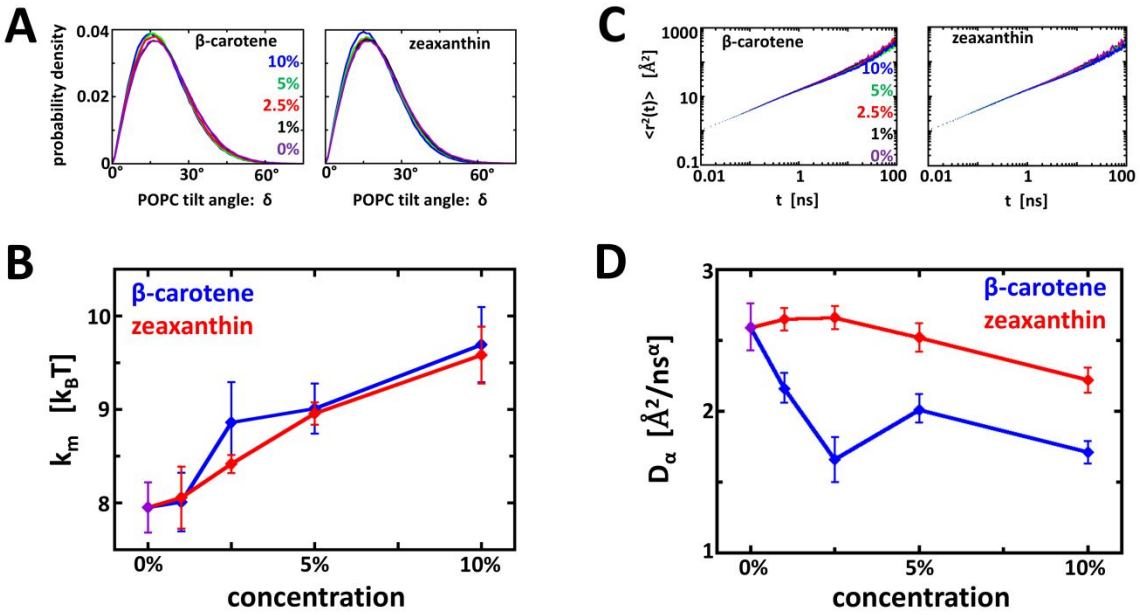

Figure 5. Membrane rigidity and lipid dynamics. (a) Distributions of POPC tilt angles at different concentrations of β-carotene (left) and zeaxanthin (right). (b) Bending modulus of the membrane as a function of β-carotene (blue) or zeaxanthin (red) concentration. (c) In-plane mean-squared displacement (MSD) as a function of time interval t averaged over all lipids for each system. (d) Anomalous diffusion coefficient D_α obtained from fits to the MSD at long time intervals (10 ns < t < 50 ns). For all membrane systems, the fitted value for α in the same time interval is 0.7 - 0.8.

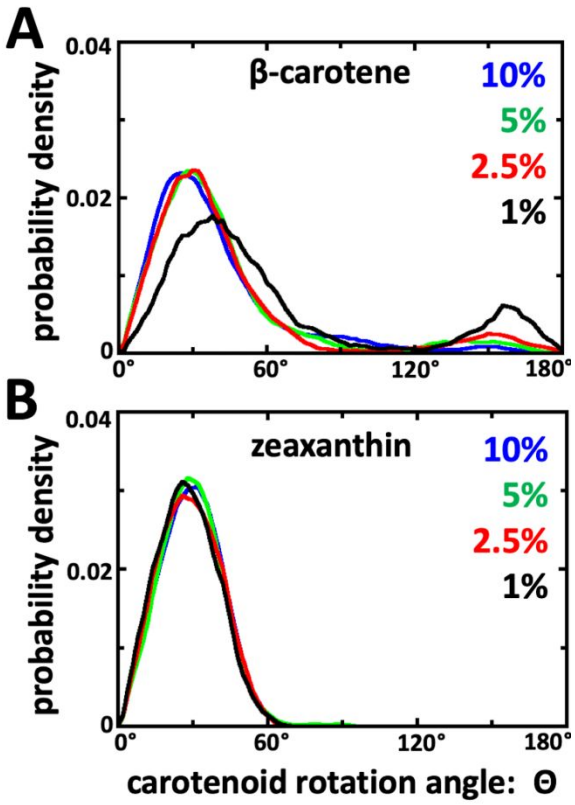

Figure 6. Carotenoid orientations. Distributions of (a) β-carotene and (b) zeaxanthin rotation angles at different concentrations. The distributions are normalized by the carotenoid concentration. Note the occurrence of large β-carotene rotation angles (i.e., >90°), which indicate flipping.

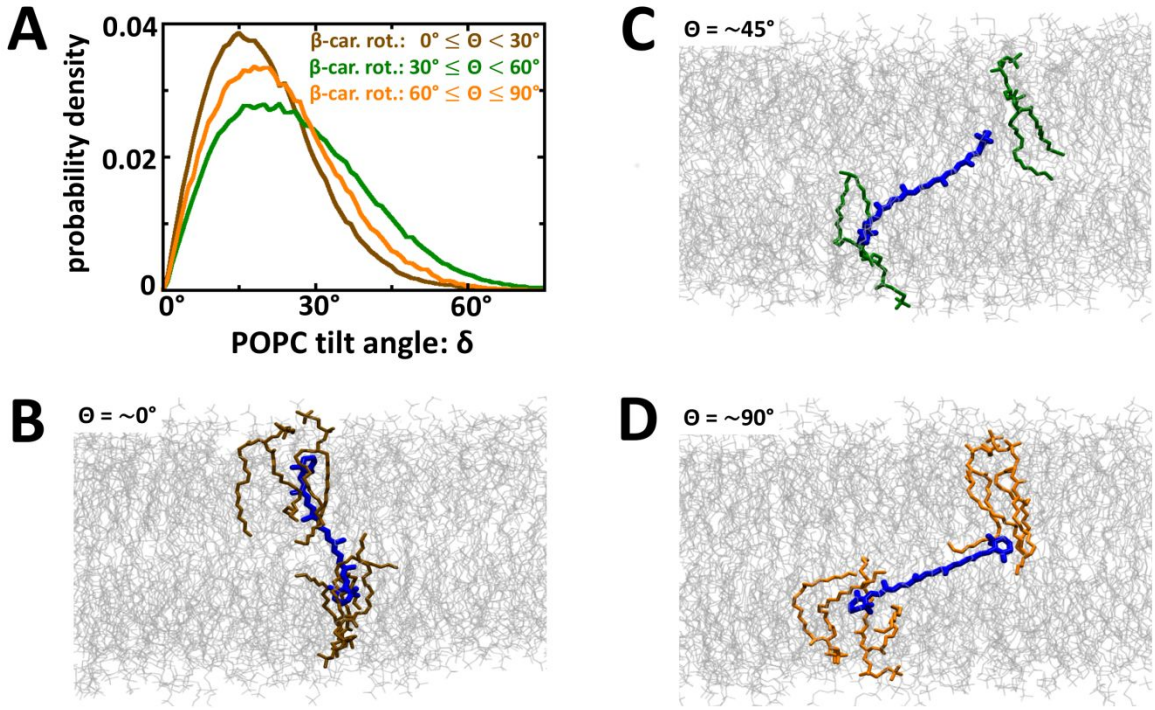

Figure 7. β-carotene rotation impacts lipid tilting. (a) Distribution of POPC tilt angles at different rotation angles of the nearby β-carotene (i.e., within 4 Å of the ionone rings) over all simulations at 4 different β-carotene concentrations. Due to the symmetry in flipping rotations, the carotenoid rotation angle is only given up to 90°, thus, for instance, the distribution with $0^o \leq \Theta < 30^o$ also includes all instances for which $150^o < \Theta \leq 180^o$. (b-d) Representative snapshots of one β-carotene along with nearby POPC molecules from the simulation at 1 mol% concentration for β-carotene rotation angles at (b) ~0°, (c) ~45°, and (d) ~90°.

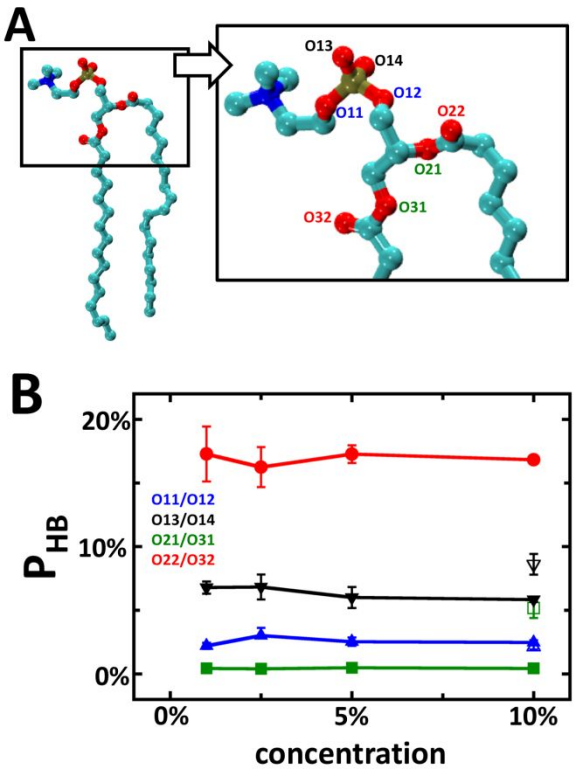

Figure 8. Zeaxanthin H-bonds to lipid head groups. (a) A ball-and-stick model of the POPC lipid (heavy atoms shown). Individual oxygens of the polar head group are labeled. (b) Zeaxanthin-POPC H-bond occupancy as a function of zeaxanthin concentration (filled symbols). This is the time and ensemble average of H-bonds between zeaxanthin hydroxyl and the POPC O11/O12 (blue upward triangles), O13/O14 (black downward triangles), O21/O31 (green squares), and O22/O32 (red circles) pairs. The corresponding empty symbols are the H-bond occupancies with an ether lipid at 10 mol% zeaxanthin. H-bonds are defined by the standard geometrical criterion of donor−acceptor distance smaller than 3.5 Å and the hydrogen−donor−acceptor angle smaller than 60°.

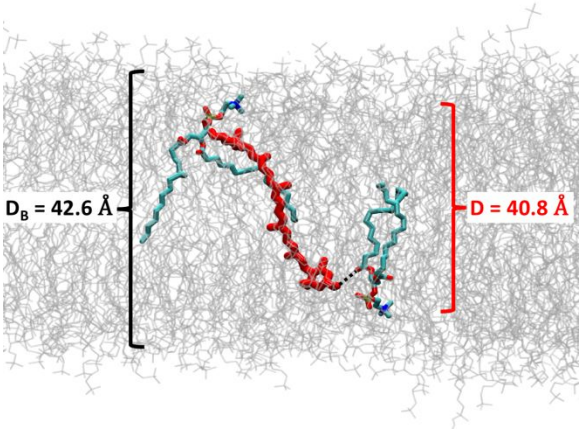

Figure 9. Zeaxanthin H-bonding reduces local bilayer thickness. A representative snapshot of one zeaxanthin molecule (red) from the simulation at 10 mol% concentration H-bonded to POPC lipids in the opposing leaflets as indicated by the dashed lines. The left bracket indicates the average bilayer thickness and the right bracket indicates the average "thickness" for the simultaneously H-bonded lipids only.